Six Degree-of-Freedom Haptic Simulation of a Stringed Musical Instrument for Triggering Sounds

Dangxiao Wang, *Senior Member, IEEE*, Xiaohan Zhao, Youjiao Shi, Yuru Zhang, *Senior Member, IEEE*, Jing Xiao, *Fellow, IEEE*

Abstract—Six degree-of-freedom (DoF) haptic rendering of multi-region contacts between a moving hand avatar and varied-shaped components of a music instrument is fundamental to realizing interactive simulation of music playing. There are two aspects of computational challenges: first, some components have significantly small sizes in some dimensions, such as the strings on a seven-string plucked instrument (e.g. Guqin), which makes it challenging to avoid pop-through during multi-region contact scenarios. Second, deformable strings may produce high-frequency vibration, which requires simulating diversified and subtle force sensations when a hand interacts with strings in different ways. In this paper, we propose a constraint-based approach to haptic interaction and simulation between a moving hand avatar and various parts of a string instrument, using a cylinder model for the string that has a large length-radius ratio and a sphere-tree model for the other parts that have complex shapes. Collision response algorithms based on configuration-based optimization is adapted to solve for the contact configuration of the hand avatar interacting with thin strings without penetration. To simulate the deformation and vibration of a string, a cylindrical volume with variable diameters is defined with response to the interaction force applied by the operator. Experimental results have validated the stability and efficiency of the proposed approach. Subtle force feelings can be simulated to reflect varied interaction patterns, to differentiate collisions between the hand avatar with a static or vibrating string and the effects of various colliding forces and touch locations on the strings.

Index Terms—Haptic rendering, strings, multi-region contact, musical instrument

1 Introduction

INTERACTIVE simulation of music instrument playing requires high-fidelity modeling and simulation to realize synchronous haptic-visual-audio multi-modal feedback. To achieve this goal, six degree-of-freedom (DoF) haptic rendering of multi-region contacts between a moving hand avatar and varied-shaped components of the instrument is a fundamental requirement.

As an example, Fig. 1 shows a seven-string plucked instrument, Guqin. Guqin playing is characterized by the following:

- Hybrid shapes: Guqin consists of a body with a complex shape of concave and convex geometric details as well as strings, each of which has significantly small size in two dimensions and a large length-radius ratio greater than 1000.
- Different contact scenarios: including single-region contact between the hand and a string, multiple-region contacts between the hand and the body/strings, and hybrid contacts between the hand and both the body and the string(s) simultaneously.
- Diversified interaction behaviors [1]: different contact speeds may lead to different interaction forces and different deformation/vibration of a string; varied contact locations may produce different responses of the string (vibration, sound); different relative motion patterns (vertical tapping, lateral sliding, cross-string sliding etc.) of the hand avatar may produce different responses of the string (vibration, sound).

Fig. 1 A seven-string plucked instrument (Guqin) and an enlarged view of a hand interaction scenario

1.1 Related work

There are several papers on haptic simulation of playing music instruments, including violin, guitar and drum playing. Berdahl introduced the concept of a virtual acoustic drum using a modular physical modeling framework. Using real-time simulation to compute force feedback and output sound, the drum can be felt, played, and heard [2]. Ren *et al.* present a virtual instrument system that enables multiple users to simultaneously perform musical pieces together on a multi-touch interface [3][4]. It can interpret user inputs and generate excitation information for real-time sound simulation to create realistic sounds depending on striking position, impact vigor, instrument shapes, and instrument cavity.

- *Dangxiao Wang, Xiaohan Zhao, Youjiao Shi, Yuru Zhang are with the State Key Lab of Virtual Reality Technology and Systems, Beihang University, No. 37 Xueyuan Road, Haidian District, Beijing 100191, China. E-mail: hapticwang@buaa.edu.cn, yuru@buaa.edu.cn*
- *Jing Xiao is with Department of Computer Science, University of North Carolina- Charlotte, USA. E-mail: xiao@uncc.edu*

Different from the above literature, the goal of this paper is to simulate playing music instrument using haptic devices. To achieve this goal, it requires collision detection between the moving tool and the music instrument in the virtual world, and simulation of 6-dimensional (6-D) force/torque feedback and corresponding response of the music components.

One technical challenge is how to avoid pop-through under diversified contact scenarios with thin-sized objects, such as strings on violin, guitar, and Guqin etc. Collision detection and response method should prevent penetration and pop-through of the tool under various hitting speeds, deformation, and vibration of the instrument. Furthermore, feelings of versatile force consisting of repulsive and vibration forces need to be simulated to reflect fine motion patterns. Lastly, music sound and visual display of small-magnitude vibration of the hitting string needs to be simulated in synchronization.

Some approaches have been proposed to tackle those challenges in 6-DoF haptic rendering, including the penalty-based approaches [5][6][7] and constraint-based approaches [8][9][10].

Modeling and simulation of interaction with thin objects has also been studied in literature. Choi and Lee modeled the haptic interaction between a rigid body tool with a polyhedral shape and a flexible thin wall [11]. The method can simulate normal and friction forces, but it is difficult to extend the method to simulating multi-region contact states in 6-DoF haptic rendering scenarios. Guidewire and surgical threads are typical thin objects. Guidewire is normally modeled as a series of finite-element beams [12]. Tang *et al.* presented a real-time physically based hybrid modeling approach to simulating guidewire insertions [13]. The long, slender body of the guidewire shaft is simulated using nonlinear elastic Cosserat rods. While the approach computed intrinsic dynamic behaviors of guidewire interactions within vascular structures, its performance on haptic rendering integrated with a haptic device remains to be validated. Lenoir *et al.* used dynamic splines to model surgical threads [14], which effectively simulated realistic bending effects of surgical threads.

In our previous work, we introduced a configuration-based optimization approach to simulating 6-DoF haptic interaction between complex-shaped rigid and deformable objects [15][16]. In this approach, the avatar controlled by the haptic device in the virtual environment is called the *haptic tool*, and its graphic display is called the *graphic tool*. As the haptic tool moves to interact with objects in the virtual environment, the approach solves for the corresponding contact configurations of the graphic tool without penetration into the other objects through constrained optimization. In this approach, both the tool and the objects are modeled by sphere-trees. The sphere-tree model is inefficient to model long and thin objects such as strings that have extremely small values in two dimensions.

Although high-fidelity or realism could be crucial in some applications such as training professional musicians, and design/fabrication of musical instruments, the main purpose of the work presented in this paper is for entertainment, i.e. for virtual musical instrument playing using haptic-visual-auditory feedback. Thus, it is not essential to achieve very high fidelity in simulation. Our simulation model aims to provide stable haptic feedback with 1kHz update, along with multi-region non-penetration contacts between the moving tool and thin objects such as strings. In addition to these requirements, the simulation model provides reasonable realism by differentiating different force sensations under varied interaction behaviors such as colliding velocity, colliding location on the string, interaction mode, and physical property of the string etc.

1.2 Contributions and organization of this paper

Contributions of this paper can be summarized in two aspects. In our previous work, we proposed a configuration-based optimization approach for 6-DoF haptic simulation of multi-region contacts and force/torque feedback. In this paper, we extend the approach to interactions involving string-shaped objects without penetration and with stability. The novelty of the proposed work is to introduce different primitives for modeling objects of different shapes, and thus to ensure simultaneous multi-region contacts between a complex-shaped moving tool and objects of different shape models (i.e. for string-shaped and complex-shaped objects). The string can be either a static or a vibrating object. This capability may be used for simulating complex haptic interaction with pipes and cables in a cluttered environment such as an aircraft carbin.

Secondly, an efficient model is introduced to simulate the multi-modal response of strings under diverse interaction behaviors. The proposed vibration model for strings takes into account several issues, including the effect of string material, vibration status of the strings, contact location, and hitting speeds etc., to facilitate simulation of subtle force feelings under different kinds of interaction.

The remainder of this paper is organized as follows. In Section 2, we present our approach. In Section 3 and Section 4, we describe experiments to validate the proposed method, including interactions between a bunny and lines/pillars, and interactions between a hand avatar and a music instrument. Finally, we present conclusions and future work in Section 5.

2 Six DoF Haptic Rendering Approach

2.1 Framework of the approach

The flowchart of the simulation approach is illustrated in Fig. 2, which includes two parts: offline modeling and online simulation.

Two different models are used to represent the main body of an instrument, which is of a complex shape, and the strings respectively. Accordingly, two algorithms of collision detection (in two branches) are used. The one involving strings identifies the index of the active string among the seven strings, contact location, and hitting speed. Next, two algorithms based on the configuration-

This article has been accepted for publication in a future issue of this journal, but has not been fully edited. Content may change prior to final publication. Citation information: DOI 10.1109/TOH.2016.2628369, IEEE Transactions on Haptics

based optimization approach [15] are used to compute the contact configuration of the hand avatar for interacting with the body and the strings of the instrument respectively, using different constraint matrices. The details will be explained in Section 2.4.

After computing the configuration of the hand avatar, feedback force and torque is computed by considering the interaction effect of repulsive force and vibration force. Finally, the response of the string is computed.

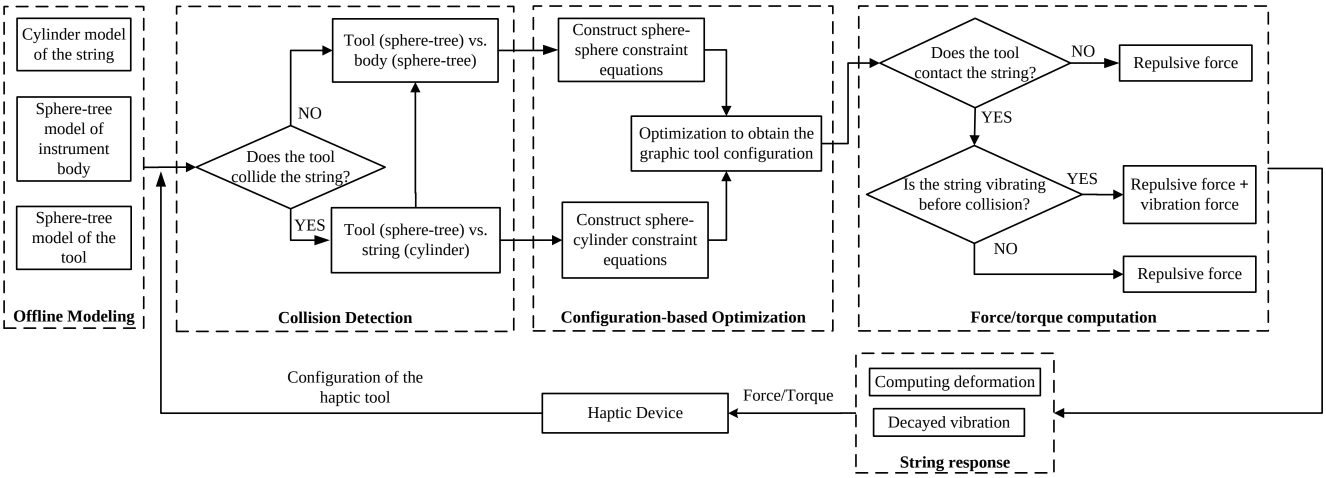

Fig. 2 Flowchart of the haptic simulation approach

2.2 Modeling

We focus on simulating music play as the result of interaction between a hand and a string instrument. The hand avatar in the virtual environment is modeled by a sphere-tree, as shown in Fig. 3. The string music instrument is represented by a sphere-tree model for its body, and the strings are represented by cylinder models. In Fig. 4, we show the triangle mesh model and sphere-tree model of the body of the music instrument.

For both the hand and the music instrument, the triangle mesh model is used for graphic rendering.

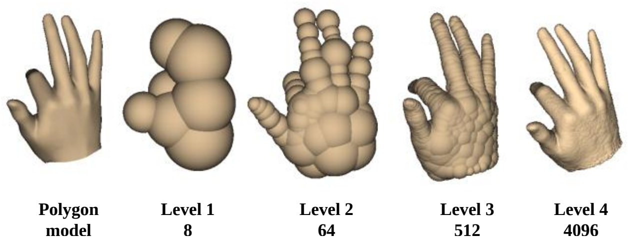

Fig. 3 Triangle mesh model and the sphere-tree models for the hand avatar

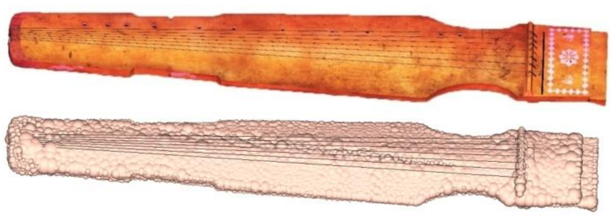

Fig. 4 The triangle mesh model and the hierarchical sphere-tree model for the body of a Guqin

To simulate the deformation and vibration of the string during interaction process, a vibrating string is modeled by a cylinder with a variable diameter as shown in Fig. 5, while the value of the diameter is computed by the deformation models to be detailed in Section 2.6. According to the theory of string vibration, the magnitude of higher-order vibrational modes is much smaller than the lowest-order vibrational mode. Therefore we ignore the effect of higher-order vibrational modes in the simulation model shown in Fig. 5.

To simulate the vibration of the string, the cylinder model is dynamically updated to represent its deformation under vibration.

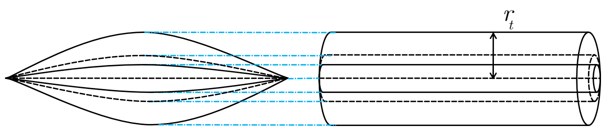

Fig. 5 Illustration of a dynamically updated model of the string

2.3 Collision Detection involving Strings

In order to detect collisions between the virtual hand and a string, information about the active string index, location of the contact/hitting point on the string, and hitting speed against the string are needed.

We introduce a discrete collision detection method to detect the collision pairs between the sphere-tree of the virtual hand and the cylinder model of a string.

Fig. 6 shows the hierarchical collision detection process, while the red spheres are detected to be in collision with the cylinder.

In above process, the key step is to detect the possible collision between a leaf sphere and the cylinder. There are two possible cases as shown in Fig. 7. Suppose the sphere center is $O(x_T, y_T, z_T)$, the sphere radius is r_T, the centers of the top and bottom surface of the cylinder are $A(x_A, y_A, z_A)$ and $B(x_B, y_B, z_B)$. The cylinder radius is r_c.

This article has been accepted for publication in a future issue of this journal, but has not been fully edited. Content may change prior to final publication. Citation information: DOI 10.1109/TOH.2016.2628369, IEEE Transactions on Haptics

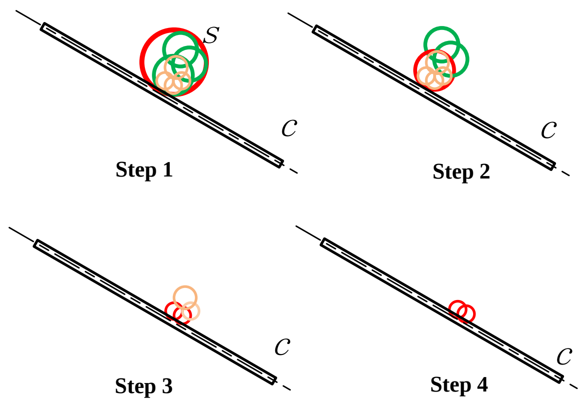

Fig. 6 Collision detection between a sphere-tree and the cylinder (S and C denote sphere-tree and cylinder respectively)

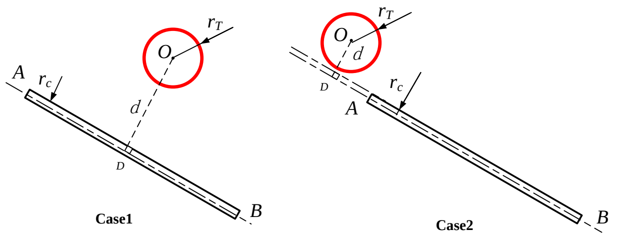

Fig. 7 Collision detection between a sphere and the cylinder

The collision occurs under the following condition:

$$d^2 \le (r_T + r_c)^2 \quad (1)$$

where d represents the distance from the center of the current sphere to the axis of the cylinder, and it can be quickly computed by the following model:

$$d^2 = \begin{vmatrix} y_T - y_A & z_T - z_A \\ y_B - y_A & z_B - z_A \end{vmatrix}^2 + \begin{vmatrix} z_T - z_A & x_T - x_A \\ z_B - z_A & x_B - x_A \end{vmatrix}^2 + \begin{vmatrix} x_T - x_A & y_T - y_A \\ x_B - x_A & y_B - y_A \end{vmatrix}^2 \quad (2)$$

where (x_A, y_A, z_A), (x_B, y_B, z_B) and (x_T, y_T, z_T) are the coordinates of the points A, B and the sphere center.

As shown in case 2 of Fig. 7, the above model does not consider the case when the projection point $\boldsymbol{D}$ moves beyond the length of the cylinder, therefore the following additional criterion is defined:

$$\lambda = \alpha \cdot \frac{|DA|}{\sqrt{(x_B - x_A)^2 + (y_B - y_A)^2 + (z_B - z_A)^2}} \quad (3)$$

where $|DA|$ represents the distance from the projection point $\boldsymbol{D}$ to the center $\boldsymbol{A}$ of the top surface of the cylinder. α equals to 1 if the point $\boldsymbol{D}$ locates to the right side of point $\boldsymbol{A}$; otherwise it equals to -1.

Therefore, the criteria for effective collisions between the sphere and cylinder are defined as

$$\begin{cases} d^2 \le (r_T + r_c)^2 \\ \lambda \in [0,1] \end{cases} \quad (4)$$

It should be noted the above collision detection criteria may introduce an approximation, i.e. if λ is slightly negative, then it should still be possible for the sphere to touch the cylinder. In order to prevent this approximation from distorting perception of the string at the end, a small margin could be introduced to enlarge the range of λ in the criteria.

As mentioned in Section 2.2, the diameter of the cylinder may dynamically change to simulate the vibration of the string during interaction.

2.4 Configuration-based optimization

We propose the following configuration-based optimization model to support the 6-DoF haptic simulation of multi-region contacts and force/torque feedback for hybrid environments involving string-shaped objects:

$$\begin{cases} Minimize: \frac{1}{2}\left(\mathbf{q}_g^t - \mathbf{q}_h^t\right)^T \mathbf{G}\left(\mathbf{q}_g^t - \mathbf{q}_h^t\right) \\ \begin{cases} C_i(x_i, y_i, z_i) \ge 0, i = 1, 2, \cdots, M \\ D_j(x_j, y_j, z_j) \ge 0, j = 1, 2, \cdots, N \end{cases} \end{cases} \quad (5)$$

As shown in Fig. 8, $\mathbf{q}_h^t$ refers to the configuration of the haptic tool in current simulation loop [15]. $\mathbf{q}_g^t$ refers to the configuration of the graphic tool, which is the solution of the quadratic programming problem with inequality constraints. Matrix $\mathbf{G}$ refers to the diagonal stiffness matrix [15]. $C_i(x_i, y_i, z_i)$ is the constraint condition for modeling non-penetration between sphere-tree models of the tool and objects [15], and x_j, y_j, z_j refers to the world coordinate of the center of the *j-th* sphere in the tool's sphere-tree. $D_j(x_j, y_j, z_j)$ refers to the constraint condition for modeling non-penetration between the sphere-tree model of the tool and the cylinder model of a string-shaped object.

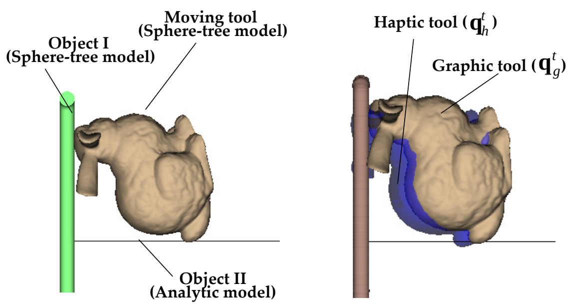

Fig. 8 Optimization under multi-region contacts with hybrid models

The non-penetration constraint between a sphere and a cylinder can be represented as the following inequality

$$d_j^2 - (r_j + r_c)^2 \ge 0, j = 1, 2, \cdots, N \quad (6)$$

where d_j refers to the distance from the j-th sphere's center to the axis of the cylinder, N refers to the number of intersected spheres with the cylinder, and r_j refers to the radius of the j-th sphere.

Because the cylinder is fixed in the virtual environment, the cylinder's axis and radius have constant values. And thus the above formula only contains one variable, i.e., the sphere's center.

$$D_j(x_j, y_j, z_j) \ge 0, j = 1, 2, \cdots, N \quad (7)$$

The constrained optimization model in (5) is solved by an active set method [19] to obtain the contact configuration of the graphic tool. The active set method is generally one of the most effective methods for small- to medium-

This article has been accepted for publication in a future issue of this journal, but has not been fully edited. Content may change prior to final publication. Citation information: DOI 10.1109/TOH.2016.2628369, IEEE Transactions on Haptics

scale QP problems, which performs well in our algorithm.

2.5 Force modeling

When the hand avatar interacts with a static string, the force/torque is computed using a 6-dimensional spring-force model [15]. When the hand avatar collides with a vibrating string, the human operator may feel both the repulsive force and a vibration force caused by the residual vibration. The force model consisting of the repulsive force $\mathbf{F}_r$ and vibration force $\mathbf{F}_v$ is defined as follows

$$\mathbf{F}_d = \mathbf{F}_r + \mathbf{F}_v \tag{8}$$

where the first term on the right side is the 3-dimensional force component in the 6-dimensional spring-force model [15], and the second term denotes a decaying component caused by the residual vibration of the string:

$$\mathbf{F}_v = k_v \cdot \mathbf{r}_{\max} \cdot e^{-\frac{t}{T_d}} \sin(\omega t) \tag{9}$$

where k_v represents the elastic restitution coefficient of the string, which models the quasi-linear relationship between the elastic restitution force and the elastic vertical deformation of the string, $\mathbf{r}_{\max}$ refers to the radius of the string's cylinder model corresponding to the maximal deformation of the string when it was released, T_d refers to a constant variable to define the decaying rate of the string, and ω denotes the angular velocity, which reflects the influence of the inherent vibration period of the string.

2.6 Collision response of the string

Under a typical interaction scenario, the string is deformed to a specific magnitude by an external force, and vibrates after the hand releases the string.

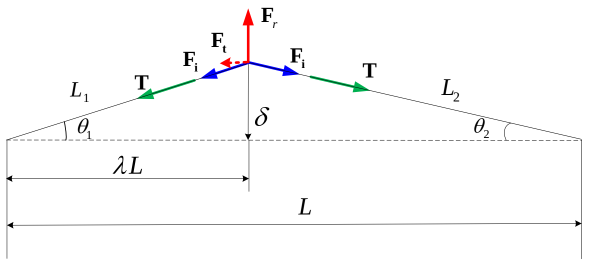

Fig. 9 Illustration of the external and internal force on the string

As illustrated in Fig. 9, the following force balance model [1] was adopted to model the relationship between the deformation of the string and the magnitude of the repulsive force $\mathbf{F}_r$, i.e.

$$\|\mathbf{F}_r\| = (\|\mathbf{T}\| + \|\mathbf{F}_i\|)(\sin\frac{\delta}{L_1} + \sin\frac{\delta}{L_2}) \tag{10}$$

where δ denotes the vertical deformation of the string. $\mathbf{T}$ refers to the pre-tension force of the string, and $\mathbf{F}_i$ refers to the internal axial force, which is computed by

$$\|\mathbf{F}_i\| = EA\left(\frac{L_1 + L_2 - L}{L}\right) \tag{11}$$

where E refers to the Young's Modulus. A refers to the sectional area of the string. L refers to the initial length of the string. L_1 and L_2 represent the actual length of the left and right part of the string respectively, which can be computed as

$$\begin{cases} L_1 = \sqrt{(\lambda L)^2 + \delta^2} \\ L_2 = \sqrt{\left[(1-\lambda)L\right]^2 + \delta^2} \end{cases} \tag{12}$$

where λ describes the relative distance from the contact point to the end point of the string.

In our simulation model, the deformation of the string is computed as proportional to the displacement of the haptic device after the collision occurred, i.e.,

$$\delta = \frac{\|\mathbf{p}_g^t - \mathbf{p}_h^t\|}{k_s} \tag{13}$$

where $\mathbf{p}_g^t$ and $\mathbf{p}_h^t$ denote the positional components of the configuration variables of the graphic tool and the haptic tool respectively. Parameter k_s denotes the scaling coefficient, which is defined to address the limited stiffness of the associated haptic device, i.e. to map the displacement of the haptic device into a much smaller deformation of the string. In our system, the scaling coefficient is defined as the ratio of the elastic restitution coefficient of an ideal string to the achievable stiffness of the Phantom device. It should be noted that the value of δ increases to its maximum at the moment when the plucking is over, and this value was defined as the maximum radius of the cylinder model. To simplify the force model, we ignore the lateral force $\mathbf{F}_t$ caused by the slight difference between the angle θ_1 and θ_2, because the lateral force could be very small.

The radius of the string may increase to a maximum value when a user presses the string, and decay in a way expressed in Eq. (9) after the user releases the string. As modeled in Eq. (10) and (13), the deformation or the radius of the string is determined by both the plucking force and the plucking locations along the axis of the string.

In order to show the visual effect of string vibration, an enlarged cylinder with a changing diameter is displayed visually. In a typical music instrument, different strings may produce different tones. For the Guqin considered in this paper, there are seven recorded tunes to be defined for the seven strings. When a string is played, the corresponding tone is played. The magnitude of the tone sound is also proportional to the interaction force $\mathbf{F_d}$. The DirectSound SDK is utilized to play the sound. This method can maintain that the haptic loop is not disturbed.

3 Interaction with Hybrid Models

A Phantom Premium 3.0 6DoF is utilized as the haptic device to provide 6-dimensional forces/torques. The specifications of the computer are: Intel(R) Core(TM) 2 2.20GHz, 2GB memory, X1550 Series Radeon graphic card. Note that no GPU is used.

The purpose of this experiment is to validate whether the proposed method can maintain non-penetration and force/torque stability under diverse contact states. The

This article has been accepted for publication in a future issue of this journal, but has not been fully edited. Content may change prior to final publication. Citation information: DOI 10.1109/TOH.2016.2628369, IEEE Transactions on Haptics

scene of the experiment is shown in Fig. 10. The tool is a moving bunny, which interacts with an object including two lines, two static pillars and a static base plate. The pillars and the base plate are modeled as sphere-tree models while the two lines are modeled as cylinders. In this experiment, the lines are regarded as rigid bodies without vibration.

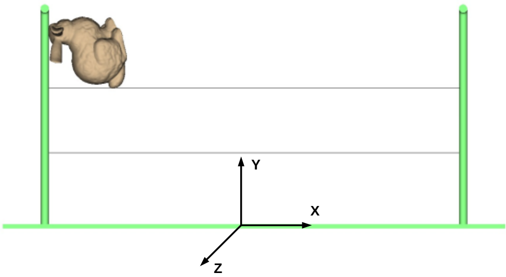

Fig. 10 A bunny interacting with the object with two pillars, two lines and a base plate.

3.1 Results under different contact states

We have tested different contact scenarios between the bunny and different parts of the object. In all cases, there was no-penetration and no pop-through between the bunny and the object. The force/torque curves were continuous, and the stability of the haptic device was maintained. Fig. 11 shows the contact scenario and force/torque signals under a single-region contact state.

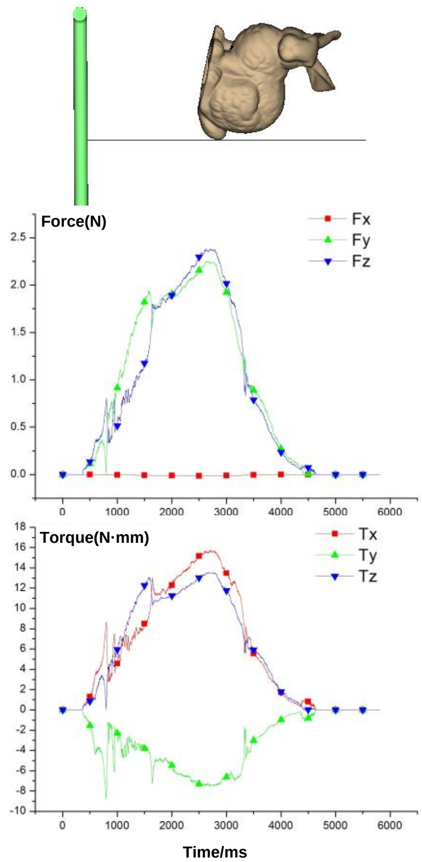

Fig. 11 A single-region contact

Fig. 12 shows the contact scenario and force/torque signals under different multi-region contact states. In a) the bunny contacts a line at two regions. In b) the bunny simultaneously contacts one line and one pillar. In c), the bunny contacts two lines simultaneously. As shown in Fig. 11 and 12-c), compared with the multi-region contacts, the torque signal under the single-region contact was significantly small. Furthermore, the torque about the y-axis was large, which illustrated the resistance torque produced by the rotation of the bunny between two strings.

a) Contacts with a line

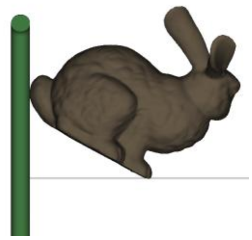

b) Contacts with line and pillar

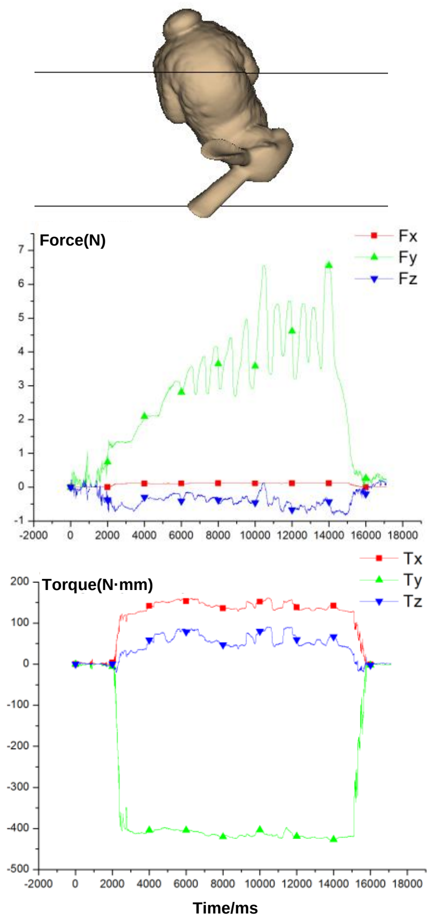

c) Contacts with two lines

Fig. 12 Multi-region contact states

3.2 Results of contact switches

Fig. 13 shows a sequence of haptic interaction, where contact switches occur. In the first phase, the moving bunny first contacts the pillar, maintains the contact and moves along the surface of the pillar, and suddenly switches to contact with the line (under constraints between the sphere-tree and cylinder models). The force F_x changes to zero at a specific time step, which is the switch time

This article has been accepted for publication in a future issue of this journal, but has not been fully edited. Content may change prior to final publication. Citation information: DOI 10.1109/TOH.2016.2628369, IEEE Transactions on Haptics

between the two contact states. During the switch process, the interaction is stable.

In the second phase, the bunny moves along a reversed trajectory, i.e. first contacts the line, maintains the contact, and moves along the line, and suddenly switches to a contact with the pillar. During the switch process, the interaction is also stable.

Detailed interaction process of this experiment is shown in the video provided online.

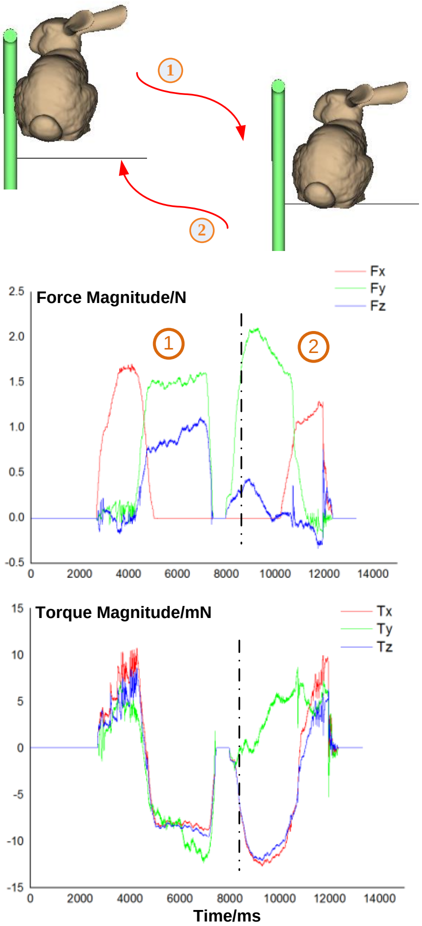

Fig. 13 Contact switches between the bunny and the objects

4 Experiments on Music Playing

As shown in Fig. 14, a user manipulates the haptic device (Phantom Premium 3.0 6DoF) to drive a virtual hand avatar to interact with a virtual Guqin. An ear-phone is used to provide the sound feedback.

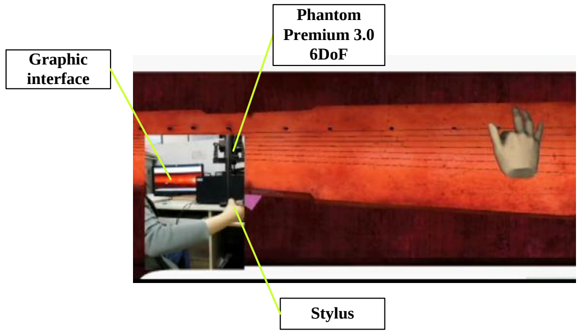

Fig. 14 Interaction scenario of the music instrument play

4.1 Results during typical playing phases

Fig. 15 shows a typical sequence of playing Guqin using the right index finger, which include 5 phases.

As shown in Fig. 15-a, the first phase of playing the Guqin is that the index finger of the hand avatar slides along the surface of the Guqin' body without touching the strings. During this phase, the force curves are smooth, and the haptic interaction is stable.

Fig. 15-b shows the second phase of playing the Guqin, which is to press a string via the index fingertip. During this procedure, the force curves remain continuous and smooth. It should also be noted that the feedback force emerges to a maximum value in the y direction (the green curve), which means that the string provides the avatar an upward resistance force when being tapped.

The third phase shown in Fig. 15-c is that the index finger goes beneath a single string and lifts it. The force curves still remain continuous, and a maximum feedback force in the y direction is produced. Contrast to phase 2, the feedback force here in the y direction turns to be negative, because the finger taps the string from bottom to top.

In the fourth phase for playing the Guqin, the fingertip quickly slides across several strings as shown in Fig. 15-d. The results indicate that the string remains vibrating when the collision is over. Correspondingly, there is vibration on the force curves, which is caused by the superposition of the string's vibration force on the repulsive force. The results show that such vibration is convergent and would not lead to instability of the interaction system.

In the fifth phase as shown in Fig. 15-e, the finger slides along a single string and maintains continuous contact. The force curves return to being continuous, and the interaction is stable.

The five steps consist of the complete procedure for playing the Guqin. The results described above indicate that the virtual Guqin system, which is based on the hybrid model, can achieve stable force feedback during the simulation. During the whole period of interaction, the haptic rendering time, including the collision detection and collision response, is less than 1ms in most phases. Besides, the algorithm can successfully prevent the avatar hand from popping-through the string even under extreme cases as shown in Fig. 16.

4.2 Results under different playing behaviors

Figure 17 illustrates the difference between two cases when the virtual hand touches a static or vibrating string. As shown in Case 1, when touching a static string, the F_y

This article has been accepted for publication in a future issue of this journal, but has not been fully edited. Content may change prior to final publication. Citation information: DOI 10.1109/TOH.2016.2628369, IEEE Transactions on Haptics

and F_z force values rises continuously and smoothly as the user gradually increases the pressure. When the avatar leaves the string suddenly, there is an abrupt drop on the force curve, and the string may keep vibrating. When the fingertip touches a vibrating string, there are a series of sawtooth signals on the F_y and F_z force curve until the string stops vibration. Due to the decaying feature of the vibration amplitude, the force curve finally resumes to be smooth.

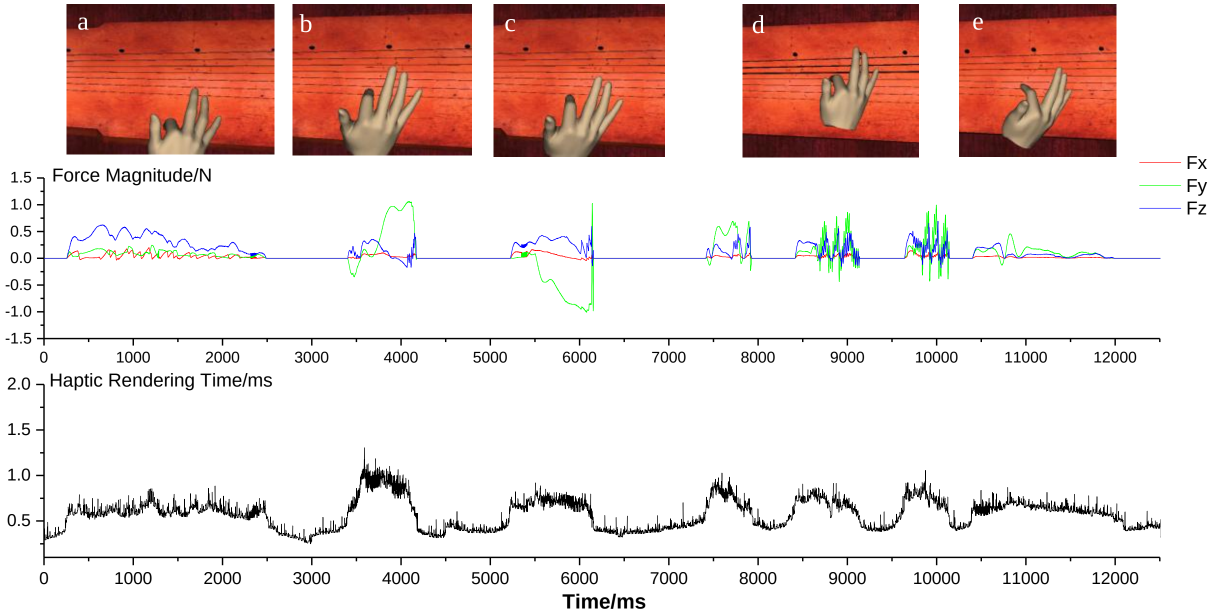

Fig. 15 Interaction force and time cost during the typical phases of playing Guqin

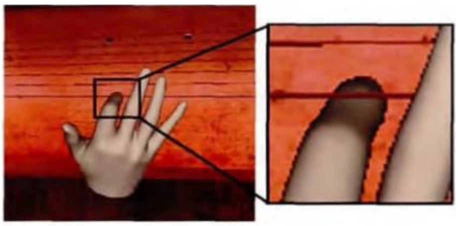

a) Sliding beneath a single string

b) Twisting between two strings.

Fig. 16 Multi-region contact scenarios with no penetration

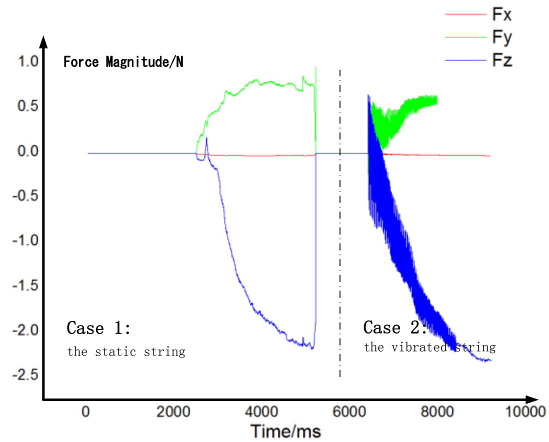

Fig. 17 Difference between tapping a static string and a vibrating string

Fig. 18 shows the results (force/haptic rendering time signal) under different contact speeds. It shows that the force curve is continuous and smooth in all speeds. No pop-through occurs even if the string is tapped with a high speed of about 1204mm/s. In addition, the time cost of haptic rendering can satisfy the requirements for stable force simulation.

The online video shows the interaction process of the music instrument playing.

This article has been accepted for publication in a future issue of this journal, but has not been fully edited. Content may change prior to final publication. Citation information: DOI 10.1109/TOH.2016.2628369, IEEE Transactions on Haptics

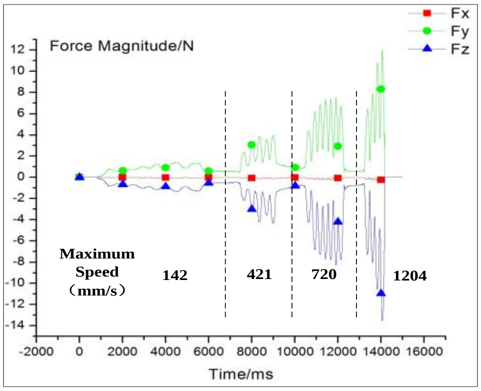

Fig. 18 The effect of different colliding speeds

4.3 Psychophysical validation of haptic sensations

Psychophysical validation was performed to evaluate whether the proposed approach can simulate diversified haptic sensations. Seven users were invited to play the virtual instrument under different experimental conditions. As mentioned in the Equation (10), the repulsive force of a Guqin's string is influenced by the physical parameters of the string including Pre-tension force T, Young's Modulus E, and Radius of the string R. Therefore, the values of each of the three parameters (Pre-tension force, Young's Modulus, Radius of the string) were tuned in three-scales (30%, 40%, 50% increment with respect to its corresponding reference value) in order to check whether participants can tell the subtle difference of haptic feeling between the increased value and the reference value. If the user could identify the difference, it validates that the proposed method is able to simulate the feeling of different strings. For example, for the Young's Modulus, the reference value was set as 1.9E11 N/m^2. A new value with 30% increment was shown and the user was required to compare the force feeling with the reference vs that with the test value, and to judge which one was stiffer. In each trial, a pair of values (consisting of a reference and a test value) was presented to the participant, and each pair was repeated for three times. Therefore, for each participant, 27 trials (3 parameters * 3 difference levels * 3 repetitions) were performed. The sequence of the target parameter and the pairs was randomly presented to the participant. For the other two parameters, the reference values were set as: T=30N and R=0.34mm.

The mean and standard deviation of the rate of correct identification from all participants are shown in Table 1. The results indicate that the rate of correct identification increased along with the increase of the difference between the test value and the reference value. One-way ANOVA shows that, for the parameter T, significant difference of the correct rate existes between the two levels (50% and 30% increment) with $F(1, 12) = 6.153$, $p=0.029$. For the three increment levels of the parameter R, significant difference existed with $F(2, 18) = 5.462$, $p=0.014$. For the three increment levels of the parameter E, no significant difference existes with $F(2, 18) = 0.064$, $p=0.938$. These results validate that the proposed model can produce different force feeling by tuning the two parameters T and R, which illustrate the capability of the proposed approach for simulating diversified haptic feeling for interactive instrument playing. The insignificant effect of tuning the parameter E might be attributed to the reason of the large initial value of the E. In future experiments, it is possible to use a smaller value of the parameter to observe its effect.

Table 1 Mean and standard deviation of the rate of correct identification for each target parameter

Target parameters	Three-scale increment between the reference and the test value		
	30% increment	40% increment	50% increment
T	47.7%± 26.5%	52.4%± 32.7%	66.7%± 27.4%
E	38.0%± 23.2%	42.9%± 37.2%	42.9%± 25.4%
R	23.7%± 25.2%	33.3%± 27.4%	62.1%± 12.9%

4.4 Preliminary user study

Four participants (2 females and 2 males) with experiences of playing Guqin were recruited to evaluate the proposed haptic simulation system. Their average age is 23, and their durations of playing Guqin ranged from 12 to 60 months with an average of 33 months. All participants gave written consent to participate in the experiment and were provided with financial compensation.

Before the formal evaluation experiment, each participant was allowed to get familiar with the Phantom haptic device using some simple demos including touch a virtual wall and a virtual sphere etc. In the evaluation experiment, the participants manipulate the device to interact with virtual strings using typical playing gestures. They were allowed to play the different strings using different contact force and different velocities, and five metrics (to be explained below) were adopted to evaluate the performance of the haptic simulation system [18]. The participants were asked to fill in a questionnaire with 100% scale to evaluate the fidelity of the haptic simulation with respect to playing real strings. It took each participant 30 minutes to perform the whole experiment.

In the following, the five metrics are explained one by one. For each metric, each participant needs to give a score after evaluation. The maximum score of 100 refers to the highest fidelity.

The first metric is the sensation of a thin string. The participants were asked to manipulate the hand-shaped avatar to collide the string with different velocities and from different approaching directions (e.g. from top or bottom side of a string), and slide around the circumference of the string while maintaining contact between the avatar and the string. The participants were asked to evaluate the haptic fidelity of interaction with a thin string, including the feeling of no penetration, small diameter etc.

The second metric is the smoothness of the string. The participants were asked to slide along the axial direction of the string and to evaluate whether the roughness of the string is sufficiently small.

The third metric is the elastic sensation, which refers to

This article has been accepted for publication in a future issue of this journal, but has not been fully edited. Content may change prior to final publication. Citation information: DOI 10.1109/TOH.2016.2628369, IEEE Transactions on Haptics

the feeling of elastic force-deformation profile of the string after pressing.

The fourth metric is the constancy of the diameter of the string. The participants were asked to slide along the axial direction of the strings and to evaluate whether the diameter of the string is constant.

The fifth metric is the feeling of the decayed vibration when interacting with a vibrating string. The participants were asked to press a string and quickly release it to produce vibration, and press it again to feel the vibration.

The quantified results of all participants are shown in Table 2. The results indicate that the proposed haptic simulation system provided a fairly realistic haptic sensation to most participants.

Table 2 Quantified evaluation results from experience players

Metrics	P1	P2	P3	P4	Mean±Std.
Thin string sensation	90	90	90	90	90 ± 0
String smoothness	100	90	95	50	83.8 ± 22.9
Elastic sensation	90	30	95	60	68.8 ± 30.1
Diameter constancy	100	60	90	90	85 ± 17.3
Decayed vibration	90	90	80	100	90 ± 8.2

The participants also provided qualified comments on the system. They commented that the virtual hand avatar could be improved to provide more typical gestures including picking, wiping, hammering, pulling, sliding etc. In the future, we plan to develop a deformable virtual hand avatar to simulate those diverse interaction gestures. The second comment was that they had to adapt their habit to get used to manipulation through the stylus of the haptic device, which degraded the haptic feeling to a large extent. They strongly suggested to manipulate the hand avatar using five fingers, and to provide the force feedback sensation directly on the fingertips. In the future, we plan to develop a haptic glove that will enable direct manipulation and provide multi-finger haptic feedback. The last comment was that the graphic display was not intuitive for finding the exact location of the strings due to the lack of the depth sensation. This could be improved by using a stereoscopic graphic display.

5 Conclusions and Future Work

To achieve interactive play of a virtual music instrument, 6-DoF haptic rendering of multi-region contacts between a hand avatar and the strings and body of the instrument is a fundamental requirement. In this paper, we have extended a constraint-based collision response algorithm and the configuration-based optimization approach to simulating contacts between the hand avatar and both the body and the strings of the instrument, using a cylinder model for the thin-sized string and a sphere-tree model for the complex shaped body of the instrument. In order to simulate the deformation and vibration of a string, the value of the cylinder diameter is varied corresponding to the real-time interaction force applied by the hand avatar.

Experimental results based on a Phantom Premium 3.0 device illustrate that the proposed method could simulate both single-region and multi-region contacts between the virtual hand and the instrument body and strings with no pop-through and no penetration. Six-dimensional force and torque were stably simulated to reflect diverse interaction behaviors.

In order to physically validate the realism of the proposed simulation model, one possible future research topic is to measure the interaction force/torque between the moving tool and the string, along with the measurement of the trajectory and velocity of the moving tool. Similar to the measurement method in [17], a force/torque sensor could be integrated into a hand-held tool, and a camera could be utilized to track the motion of the tool. Furthermore, force sensors could be embedded into the base of the instrument, or even in the string [1]. These measured data could possibly provide ground-truth to evaluate the proposed haptic rendering algorithm. In the next step, we also plan to improve the realism of the simulation by introducing deformable behavior of the finger tip in the hand avatar. Furthermore, a more intuitive haptic device such as the CyberGrasp or other haptic gloves [20] could potentially be used with the simulation system to enable a more natural music playing experience. Finally, we plan to perform more rigorous user study to evaluate the fidelity of the simulation system.

Acknowledgment

This work is supported by the National Natural Science Foundation of China under the grant No. 61572055, No. 61532003, and No. 61190125, and also partially supported by National Key Research and Development Plan under Grant No. 2016YFB1001200.

References

[1] X. Deng, Z. Yu, W. Yao, M. Chen, Dynamic analysis on Guzheng string vibration and bridge transmission, *Journal of Vibration and Shock,* Vol. 34, No. 18, 2015:166-170

[2] E. Berdahl, "An Example of Creative Physical Modeling: A Simulation of the Haptic Drum," *TEI 2013*, vol. 10, no. 13, Feb. 2013.

[3] Z. Ren, R. Mehra, J. Coposky, and M. C. Lin, "Designing virtual instruments with touch-enabled interface," *Virtual Instrument*, pp. 433-436, 2012.

[4] Z. Ren, R. Mehra, J. Coposky, and M. C. Lin, "Tabletop ensemble: touch-enabled virtual percussion instruments," *Virtual Instrument*, pp. 7-14, 2012.

[5] M. A. Otaduy and M. C. Lin, "A Modular Haptic Rendering Algorithm for Stable and Transparent 6-DoF Manipulation," *IEEE Trans. Robot.*, vol. 22, no. 4, pp. 751-762, 2006.

[6] J. Barbič and D. L. James, "Six-DoF Haptic Rendering of Contact between Geometrically Complex Reduced Deformable Models," *IEEE Trans. Haptics*, vol. 1, no. 1, pp. 39-52, 2008.

[7] W. McNeely, K. Puterbaugh, and J. Troy, "Voxel-based 6-DOF haptic rendering improvements, " *Haptics-e*, vol. 3, no. 7, 2006

[8] C. Duriez, F. Dubois, A. Kheddar and C. Andriot, "Realistic haptic rendering of interacting deformable objects in virtual environments," *IEEE Trans. Vis. Comput. Graph.*, vol. 12, no. 1, pp.36-47, 2006.

[9] M. Ortega, S. Redon and S. Coquillart, "A Six Degree-of-Freedom God-Object Method for Haptic Display of Rigid Bodies with surface properties," *IEEE Trans. Vis. Comput. Graph.*, vol. 13, no. 3, pp 458-469, 2007.

[10] I. Peterlik, M. Nouicer, C. Duriez, S. Cotin, and A. Kheddar. "Constraint- based haptic rendering of multirate compliant mechanisms," *IEEE Trans. Haptics,* vol. 4, pp. 175–187, July 2011.

[11] H. R. Choi, S. R. Lee, "Force Display System for Manipulating Thin Flexible Objects," *IEEE International Workshop on Robot and Human Communication* 1996, pp. 507-512

[12] J. Lenoir, S. Cotin, C. Duriez, and P. Neumann, “Interactive physicallybased simulation of catheter and guidewire,” *Comput. Graph.*, vol. 30, no. 3, pp. 417–423, 2006.

[13] W. Tang, T. Wan, D. A. Gould, T. How, and N. W. John, "A Stable and Real-Time Nonlinear Elastic Approach to Simulating Guidewire and Catheter Insertions Based on Cosserat Rod," *IEEE Transactions on Biomedical Engineering*, Vol. 59, No. 8, Aug. 2012, pp. 2211-2218

[14] J. Lenoir, P. Meseure, L. Grisoni, and C. Chaillou, “Surgical thread simulation,” *Model. Simulat. Comput.-Aided Med. Surg.*, 2002, pp. 102–107

[15] D. Wang, X. Zhang, Y. Zhang and J. Xiao, "Configuration-based Optimization for Six Degree-of-Freedom Haptic Rendering for Fine Manipulation," *IEEE Trans. Haptics*, vol. 6, no. 2, pp. 167-180, 2013.

[16] D. Wang, Y. Shi, S. Liu, Y. Zhang, and J. Xiao, "Haptic Simulation of Organ Deformation and Hybrid Contacts in Dental Operations," *IEEE Trans. Haptics*, vol. 7, no. 1, pp. 48-60, 2014.

[17] H. Culbertson, J. Unwin, and K. J. Kuchenbecker. Modeling and Rendering Realistic Textures from Unconstrained Tool-Surface Interactions. *IEEE Transactions on Haptics*. 7(3):381-393, 2014.

[18] F. Yang. The Physical Property Measurement of Guqin Strings [J]. *Yanyi Shebei Yu Keji*, 2014(9):46-51 (In Chinese).

[19] J. Nocedal and S.J. Wright, Numerical Optimization, Second Ed. *Springer-Verlag*, 2006

[20] I. Jo, and J. Bae, Design and Control of a Wearable Hand Exoskeleton with Force-controllable and Compact Actuator Modules, *Proc. of 2015 IEEE International Conference on Robotics and Automation (ICRA)*, Seattle, Washington, May 26-30, 2015, pp. 5596-5601

Dangxiao WANG (M’05-SM’13) received a Ph.D. degree from Beihang University, Beijing, China in 2004. Currently he is an Associate Professor at the State Key Laboratory of Virtual Reality Technology and Systems in Beihang University. From 2004 to 2006, he was a post Doc at Beihang University. From 2006 to 2007, he was an Assistant Professor in the School of Mechanical Engineering and Automation, Beihang University. His research interests include haptic rendering, NeuroHaptics and medical robotic systems. He is a senior member of IEEE. He has been the chair of Executive Committee of the IEEE Technical Committee on Haptics (IEEE TCH) since 2014.

Xiaohan ZHAO received the BE degree in mechanical design in 2014, from the School of Mechanical Engineering & Automation, Beihang University, Beijing, China. Currently he is working toward the ME degree in mechanical engineering at the Beihang University, Beijing, China. His research interests include mechanism design and haptic rendering.

Youjiao SHI received the BE degree in mechanical design in 2012, from Najing University of Aeronautics and Astronautics, Nanjing, Jiangsu Province, China. Currently she is working toward the ME degree in mechanical engineering at the Beihang University, Beijing, China. Her research interests include haptic rendering.

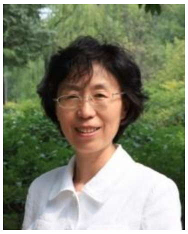

Yuru ZHANG (M’95-SM’08) received the Ph.D. degrees in mechanical engineering from Beihang University, Beijing, China in 1987. Currently she is leading the Division of Human-Machine Interaction at the State Key Laboratory of Virtual Reality Technology and System. Her technical interests include haptic human-machine interface, medical robotic system, robotic dexterous manipulation, and virtual prototyping. She is a senior member of IEEE, and a member of ASME.

Jing XIAO (S’88-M’90-SM’04-F’13) is a Professor of Computer Science, College of Computing and Informatics, University of North Carolina at Charlotte, USA. She received her PhD degree in Computer, Information, and Control Engineering from University of Michigan. Jing Xiao’s research interests include robotic manipulation and assembly, haptic rendering, and motion planning. She is a Fellow of IEEE.